

Model-Based Multi-Echo Water/Fat-Separated MR Thermometry

Megan E Poorman^{1,2}, Chris J Diederich³, Graham Sommer⁴, Kim Butts Pauly⁴, and William A Grissom^{1,2}

¹Biomedical Engineering, Vanderbilt University, Nashville, TN, United States, ²Institute of Imaging Science, Vanderbilt University, Nashville, TN, United States,

³Radiation Oncology, University of California, San Francisco, CA, United States, ⁴Radiology, Stanford University, Stanford, CA, United States

Target audience: MR scientists interested in MR thermometry.

Purpose: In recent years several advanced model-based algorithms for separating water and fat signals in multi-echo MR acquisitions have been developed ([1-3] and several others). They all improve on the conventional Dixon method [4,5] but also require significant computation times, and to our knowledge online implementations of these algorithms suitable for real-time MR thermometry have not been reported. However, there are several thermal therapies that would benefit from accurate water/fat-separated MR thermometry, such as MR-guided focused ultrasound surgery (MRgFUS) in the breast [6,7]. Furthermore, current algorithms assume a known ppm difference between water and fat, whereas water's ppm shift actually changes during heating due to the proton resonance frequency (PRF) shift with temperature, which causes temperature errors in its own estimation when it is ignored in water/fat separation [8]. We propose an efficient, model-based PRF-shift temperature reconstruction approach that leverages iterative model-based water/fat separations of baseline images acquired before heating, and fits them to subsequent dynamic images with heating to estimate water's heating-induced ppm shift. The result is an algorithm that achieves high-quality water/fat separations for PRF-shift thermometry with online-compatible compute times. The method is demonstrated in simulations and canine prostate MRgFUS experiments.

Methods: Algorithm Figure 1 illustrates the proposed method. The Berglund water/fat separation algorithm [3] is first applied to multi-echo baseline images acquired prior to heating. It fits a multipeak signal model to each voxel, returning water and fat signal amplitudes and an off-resonance and R_2^* map. A modified multipeak signal model accounting for the PRF shift of water due to heating is then fit to the subsequent dynamic multi-echo images, and is given by: $S(t_e, \Delta\omega) = (We^{i\Delta\omega t_e} + F \sum_{m=1}^M \alpha_m e^{i\omega_m t_e})e^{(i\omega - R_2^*)t_e}$, where t_e is echo time, W and F are the baseline water and fat amplitudes, M is the number of fat peaks, α_m and ω_m are the fat peak amplitudes, and ω is the baseline off-resonance map. The temperature-dependent water frequency shift $\Delta\omega(T)$ is the only unknown parameter in this model and is defined as $\Delta\omega(T) = \gamma B_0 c T$, where c is -0.01 (ppm/°C). For each dynamic a gradient descent algorithm is used to efficiently solve for $\Delta\omega(T)$ by minimizing a least-squares function that measures errors between the model and the multi-echo images.

Simulation A mixed water/fat phantom (Fig. 2a) was defined at 3 Tesla on a 128x128 matrix in MATLAB (Mathworks, Natick, MA, USA) with 9 fat peaks [3]. A Gaussian hot spot of varying amplitude and 5-voxel full-width at half-max was applied to water in mixed water/fat voxels and multi-echo images were generated over a range of peak hot spot temperatures up to 36°C. Three images were synthesized with a TE difference of 1.15 ms. Temperature maps were estimated using three-point Dixon and the Berglund algorithm at each peak temperature, as well as the proposed model-based algorithm.

In vivo MRgFUS The proposed algorithm and 3-point Dixon-based temperature mapping were applied to a multi-echo data set obtained *in vivo* during trans-urethral ultrasound ablation of a canine prostate [9] obtained on an intraoperative 0.5T GE scanner (GE Healthcare, Waukesha, WI, USA) with an endorectal coil and multi-echo sequence (TR = 150-180 ms, first TE = 14.3 ms, ΔTE = 7.15ms, 256x96 matrix size). Temperature maps were reconstructed using three-point Dixon and the proposed model-based method.

Results: Simulation Figure 2b shows temperature maps reconstructed by the three methods at peak heat. The 3-point Dixon separation failed in the middle of the hot spot, while the Berglund reconstruction underestimated it. Figure 2c plots RMS temperature errors (measured over an 11-voxel-diameter window centered on the hot spot) as a function of hot spot amplitude, and shows that the model-based temperature reconstruction achieved negligible error, while the other two methods' error grew with increasing temperature, and the Dixon error curve jumps near 24°C when the water and fat signals swapped. After the initial Berglund water/fat separation, the model-based method required an average of 0.09 s compute time per image.

In vivo MRgFUS The Dixon and proposed model-based methods produced similar temperature maps that had maximum values within 1°C of each other inside the prostate, where voxels contained only water (Fig. 3, top row). However, substantial differences appeared in mixed voxels adjacent to the hot spots containing both water and fat (Fig. 3, bottom row; mixed voxels defined as water and fat signals both greater than 10% of maximum signals). The Dixon method overestimated the temperature in those regions (maximum difference 19.2°C), consistent with previous observations of temperature map errors in mixed voxels [8]. The model-based method required an average of 0.5 s compute time per image after the initial Berglund separation.

Conclusion: We have described and validated a model-based temperature reconstruction for multi-echo acquisitions that leverages advanced water/fat separation techniques while accounting for the frequency shift of heated water, and achieving compute times that are compatible with online use.

Acknowledgments: This work was supported by DoD W81XWH-12-BCRP-IDEA, NIH RO1 CA111981, and a Vanderbilt University Discovery Grant. **References:** [1] D Hernando et al, MRM 59(3):571-580, 2008. [2] M Jacob et al, IEEE TMI 28(2):173-184, 2009. [3] J Berglund et al, MRM 67:1684-1693, 2012. [4] WT Dixon et al, Radiology 153:189-194(1984) [5] GH Glover et al MRM 18:371-383, 1991. [6] EC Gombos et al Top MRI 17(3):181-188, 2006. [7] LW Hofstetter et al JMRI 36:722-32, 2012. [8] V Rieke et al, JMRI 27:673-677, 2008. [9] V Rieke et al, IEEE TMI 26(6):813-821, 2007.

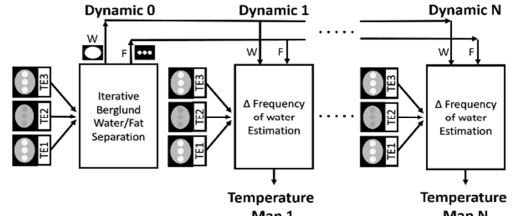


Figure 1: Model-based thermometry algorithm overview.

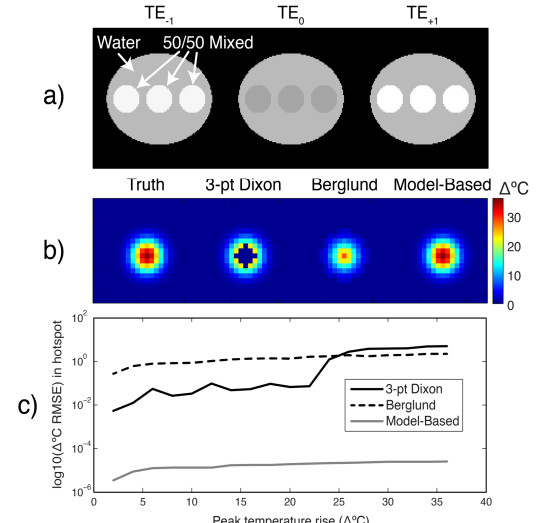


Figure 2: a) Simulated water/fat phantom at different TEs b) Reconstructed hotspot temperature maps. c) RMS hotspot error of methods on a log scale.

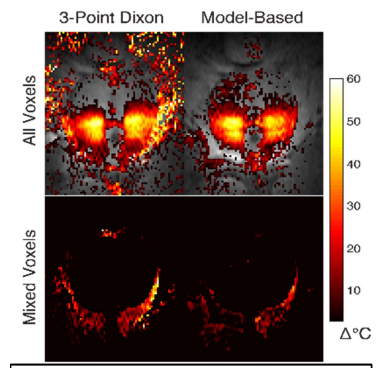


Figure 3: Prostate sonication temperature map comparison. (Top) All heating overlayed on base image (Bottom) Heating in mixed fat/water voxels only.